Correction for Missed Events Based on a Realistic Model of a Detector

Silke Draber and Roland Schultze
Institut für Angewandte Physik der Universität Kiel, D-24098 Kiel, Germany

ABSTRACT Quantitative patch-clamp analysis based on dwell-time histograms has to deal with the problem of missed events. The correction of the evaluated time constants has to take into account the characteristics of the detector used for the reconstruction of the time series. In previous approaches a simple model of the detector has been used, which is based on the assumption that all events shorter than the temporal resolution t_{res} were missed, irrespective of the preceding events. Rather than the standard assumption of a fixed dead time, we introduce a more realistic model of a detector by a continuous-time version of the Hinkley detector. The combined state of the channel and the detector obeys a Markov model, which is governed by a Fokker-Planck-Kolmogorov partial differential equation. The steady-state solution leads to the determination of the apparent time constants τ_o and τ_c depending on the true rate constants k_{oc} and k_{co} and the temporal resolution t_{res} of the detector. Simulations with different kinds of detectors, including the Bessel filter with half-amplitude threshold detection, are performed. They show that our new equation predicts the dependence of τ_c and τ_o on k_{oc}, k_{co}, and t_{res} better than the standard equation used until now.

INTRODUCTION

Limited time resolution

The patch-clamp technique (Sakmann and Neher, 1983) allows the direct observation of channels switching between open and closed states. Due to noise, however, the detector used for the analysis of the recorded pipette current has to be set to a certain temporal resolution t_{res}. The time resolution t_{res} is defined as the duration of an isolated noise-free event, which is just long enough to be detected. In the case of the Hinkley detector (Page, 1955; Hinkley, 1971; Basseville and Benveniste, 1986) and the higher order Hinkley detector (Schultze and Draber, 1993), the time resolution t_{res} is the adjustable parameter for the sensitivity of the detector. In the case of the Bessel filter with half-amplitude threshold analysis, the time resolution depends on the adjustable 3-dB frequency f_{3dB} by $t_{res} = 0.18/f_{3dB}$. In a previous paper (Schultze and Draber, 1993), we studied the optimal setting of t_{res} for different detectors depending on the properties of the noise and the signal. Of course, t_{res} must be chosen to be as short as possible, but the false alarm rate increases drastically if t_{res} is decreased under a threshold which depends on the signal/noise ratio. Setting the time resolution according to the rule of thumb

$$t_{res} = 32/SNR^2 \quad (1)$$

ensures that there will be a tolerably low number of false alarms.

Consequences on the dwell-time histograms and correction strategy

The omission of short events leads to an overestimation of the duration of the detected events. As a consequence, the time constants τ obtained from fitting the measured dwell-time histograms are longer than those that would have been obtained without dwell-time omission. Therefore, a correction for missed events has to be performed when calculating the rate constants k of the channel from the time constants τ obtained from the exponential fit of the dwell-time histograms. A theory is needed that predicts the time constants τ, given the rate constants k of the channel and the time resolution t_{res} of the detector. Numerical inversion allows the determination of k from τ and t_{res} as required in practical cases. The question of invertibility is addressed in the Discussion.

Different kinds of methods for the analysis of single-channel data

The channel gating originally produces a current that is a nearly noiseless switching between different levels. If only one channel is observed, there are normally only two levels of current, one for the closed channel and one for the open channel. The aim of single-channel analysis is to find out the kinetic scheme underlying this stochastic process of channel gating. In every patch-clamp setup, however, the current signal undergoes several changes until it is recorded digitally. First, the colored noise arising from the pipette capacity (Hamill et al., 1981) adds to the measured current. Second, the patch-clamp amplifier itself produces additional noise. Third, the signal must be low-pass filtered through an antialiasing filter, often of the Bessel type. Finally the analog signal is sampled and converted to a sequence of digital numbers, which is convenient for storing it on a computer hard disk.

Now the analysis can go different ways. One possibility is to disregard the temporal information and to look only at the amplitude histogram, the distribution of the sampled current values. The shape of this distribution allows some inference about the underlying gating model. Yellen

Received for publication 26 July 1993 and in final form 18 October 1993.
Address reprint requests to Dr. Draber.

0006-3495/94/01/191/11 $2.00

(1984) and Klieber and Gradmann (1993) have used the theory of β-distributions, which FitzHugh (1983) has developed for a two-state Markov model and a first-order filter.

We favor another concept that is more commonly used. The temporal information of subsequent gating events allows a more sophisticated analysis of the gating mechanism. Therefore, a detector is applied to reconstruct the original current record as closely as possible. The standard algorithm for such a detector is the combination of a Bessel filter and half-amplitude threshold analysis (Colquhoun and Sigworth, 1983) of the filtered signal. The application of a first-order low-pass filter instead of a fourth- or eighth-order Bessel filter gives poor performance (Schultze and Draber, 1993). Therefore, the first-order low-pass filter with threshold detection should not be used for analysis of data or for theory.

A different family of detectors is based on nonlinear filters: the Hinkley detector (Page, 1955; Hinkley, 1971; Basseville and Benveniste, 1986) and the higher order Hinkley detector (Schultze and Draber, 1993). We have shown that they give better performance than the standard Bessel algorithm (Schultze and Draber, 1993).

Analysis without correction for missed events

Colquhoun and Hawkes (1982) showed that an arbitrarily complex Markov model of gating without dwell-time omission results in dwell-time histograms that are sums of exponentials and gave general equations of how time constants τ and amplitude factors of the exponentials depend on the rate constants k of the underlying Markov model.

Brief events missed by the detector

Regardless which detector (Bessel, Hinkley, or higher order Hinkley) is applied, they all miss short events, because short events are indistinguishable from noise-induced fluctuations. Because of dwell-time omission, the reconstructed record contains less events, and the detected events are therefore longer than the events in the original channel gating.

Despite dwell-time omission the resulting dwell-time histograms can be fitted reasonably well by a shifted exponential, starting at t_{res}. The time constant, however, differs from the true time constant that would have been fitted without missed events. Many attempts to correct the results for the effect of missed events, therefore, resulted in a formula that describes for the two-state case how the time constants τ_o and τ_c of the open- and closed-time distribution depend on the time resolution t_{res} of the detector and the rate constants k_{oc} and k_{co} (Colquhoun and Sigworth, 1983; Blatz and Magleby, 1986; Yeo et al., 1988). Such functional dependence $\tau_o(k_{oc}, k_{co}, t_{res})$ is also developed in this article.

Correction methods based on the assumption of a fixed dead time

An early result, commonly used until now, goes back to Colquhoun and Sigworth (1983), who gave their equations in terms of mean values M_o and M_c for the dwell times in the open and the closed state:

$$M_o(k_{oc}, k_{co}, t_{res}) \tag{2}$$

$$= \tau_o + t_{res} = \frac{1}{k_{oc} \cdot \exp(-k_{co} t_{res})} + \frac{1}{k_{co} \cdot \exp(-k_{co} t_{res})} - \frac{1}{k_{co}}$$

$$M_c(k_{oc}, k_{co}, t_{res}) \tag{3}$$

$$= \tau_c + t_{res} = \frac{1}{k_{co} \cdot \exp(-k_{oc} t_{res})} + \frac{1}{k_{oc} \cdot \exp(-k_{oc} t_{res})} - \frac{1}{k_{oc}}$$

These mean durations are calculated under the condition that all events shorter than a fixed dead time t_{res} were missed, and all events longer than this dead time were detected. This is an intuitively appealing model for time interval omission. Though quite simple, it describes the main aspect of time interval omission and condenses the complex mathematics of noise, filtering, sampling, and detection in a single parameter. The concept of a fixed dead time provided the basis for many important papers about dwell-time omission.

Roux and Sauvé (1985) showed that the dwell-time distributions are not exactly exponential. They gave some equations for the Laplace transform of the dwell-time distributions for Markov schemes of any complexity. Blatz and Magleby (1986) developed a general concept of how to extend the two-state result of Colquhoun and Sigworth (1983) to complex Markov models by the introduction of so-called phantom states, which account for the undetected events. For the two-state case, Yeo et al. (1988) and Milne et al. (1989) showed that a maximum likelihood fit with a single (shifted) exponential confirms exactly the mean dwell times M according to Colquhoun and Sigworth (1983). Crouzy and Sigworth (1990) gave a more general approach for the extension of the two-state results to the multi-state case. They made use of Kienker's (1989) result and first transformed the gating model into an equivalent uncoupled scheme before introducing phantom states. Hawkes et al. (1990) and Jalali and Hawkes (1992) succeeded in giving analytical expressions for the dwell-time histograms for any type of Markov model. Although their numerical examples are quite extreme (more events missed than detected), the comparison of the dominant time constant (Table 1 in Hawkes et al., 1990) reveals that the various methods mentioned above have nearly identical results. This justifies the representation of all the fixed dead time theories by the fundamental Eq. 4 and the showing of the benefits of our new result (Eqs. 34 and 35) against that old equation in the Comparison section.

Ball et al. (1993) put the theory of missed events in a very general mathematical framework. All models with or without time interval omission are treated as semi-Markov models. Once the kernel of the semi-Markov model is given, their theory provides all important statistical properties of the observed dwell times: means, distributions, and correlations. Besides the mathematical clarity of this approach, it also allows the use of other than pure Markov models for the channel. Every semi-Markov model will do, for instance, a fractal model (Liebovitch, 1993).

All of the articles mentioned, from Colquhoun and Sigworth (1983) to Ball et al. (1993), continued to use the definition of a fixed dead time as a model for time interval omission. For the two-state model they all support the result of Colquhoun and Sigworth (1983), which we will call the "old" equation for missed events correction in the following.

$$\tau_c(k_{oc}, k_{co}, t_{res}) = \frac{1}{k_{oc} \cdot \exp(-k_{co} t_{res})} + \frac{1}{k_{co} \cdot \exp(-k_{co} t_{res})} - \frac{1}{k_{co}} - t_{res} \quad (4)$$

The equation for τ_c is obtained by simply exchanging the indices o and c.

In order to avoid confusion arising from the differences in the nomenclature in papers about missed events we list the most important quantities in Table 1.

Alternative approaches instead of fixed dead time

The fixed dead time assumption is not realistic for any detector, especially if both open and closed events are short, because every detector contains a sort of memory, which is a test value or a filtered value, depending on previous events. In a real detector, multiple short events can lead to a detection. They are not simply ignored.

Although many authors admit that the fixed dead time is somehow not realistic, there has been little effort to find alternatives. Roux and Sauvé (1985) have compared their exponential approximation, based on fixed dead time, with Rickard's (1977) solution. His equation is, however, only valid for a very special and unrealistic case. The channel obeys to a symmetrical ($k_{oc} = k_{co}$) two-state Markov model, no noise, first-order low-pass and half-amplitude threshold analysis. The only thorough investigation of the shortcomings due to the assumption of a fixed dead time has been carried out by Magleby and Weiss (1990). They clearly show that simulation of a realistic recording situation with noise, fourth-order Bessel filter, and threshold detection gives markedly shorter dwell times than the model of a fixed dead time. In other words, the fixed dead time exaggerates the effect of missed events, because it neglects the possibility that subsequent short events sum up to a detected event. Magleby and Weiss (1990) suggest dropping the theory built around the fixed dead time and using simulations instead. This approach is principally possible, but it takes some time on a computer to simulate the dwell-time histograms for one set of rate constants. And, for the purpose of fitting, this time-consuming simulation would have to be repeated several times.

The new theoretical approach: modeling the detector

Although the simulation approach of Magleby and Weiss (1990) gives the correct results, we are interested in finding an analytical expression that gives the dependence of the time constants τ_o and τ_c on the rate constants k_{oc} and k_{co} and the time resolution t_{res}. Such an analytical formula would offer tremendously shorter computing times compared to the repeated simulations of Magleby and Weiss (1990). It may also lead to a better understanding of the mechanisms of dwell-time omission.

Our aim in this article is to find an equation that can be substituted for the widely used old Eq. 4 without any additional parameters. This new equation (Eq. 34), which we develop in the Theory section, is not based on the unrealistic assumption of fixed dead time, but on a realistic model of a detector. Since there are different kinds of detectors, and, further, different conditions of noise and sampling frequency, which cannot be described by simply specifying t_{res}, we chose the following strategy. We derived the new equation for the Hinkley detector for no noise and in continuous time. Although this is a special case, it supplies a much better model for a detector in general than the fixed dead time approach because now the memory of the detector is adequately contained in the model. This generality is shown in the Comparison section, where we compare our new equation with results from simulations under realistic recording conditions.

THEORY

Model of the channel

We consider a two-state model with one open and one closed state:

$$O \underset{k_{co}}{\overset{k_{oc}}{\rightleftharpoons}} C \quad (5)$$

TABLE 1 Nomenclature in some publications dealing with the dwell-time omission problem

	This Article	Colquhoun and Sigworth (1983)	Blatz and Magleby (1986)	Milne et al. (1989)	Crouzy and Sigworth (1990)
True rate constants	k_{oc}	$1/\mu_o$	k_{12}	$1/\mu_X$	k_{10}
	k_{co}	$1/\mu_g$	k_{21}	$1/\mu_Y$	k_{01}
Time resolution	t_{res}	ξ_o, ξ_c	Dead time D	Dead time ξ	Dead time δ
Apparent mean dwell time	M_o	${}^e\mu_o$	$L_{obs(1)}$	μ_T	
	M_c	${}^e\mu_g$	$L_{obs(2)}$	μ_S	DM_c
Fitted time constants	τ_o		$\tau_{obs(1)}$	μ_U	
	τ_c		$\tau_{obs(2)}$	μ_V	τ_{obs}

The two-state model without dwell-time omission results in single exponentials for the dwell-time histograms. The time constant of the open-time histogram is $\tau_o = 1/k_{oc}$ and for the closed events is $\tau_c = 1/k_{co}$. Since the distributions are exponential, the time constants τ_o and τ_c are also the mean open and closed times, M_o and M_c, respectively. The two-state model is the simplest possible gating model, but throughout the history of single-channel analysis, main concepts and insights were first obtained for the two-state case and afterwards extended to more complex models. An approach to extend the application of our new Eq. 34 to more complex schemes is considered in the Discussion.

Although the problem of missed events originally arises from sampling and noise, we assumed the noise-free continuous-time case for the development of the theory. Fig. 1 *A* gives an example for a signal $z(t)$ of pipette current, which jumps between the two levels μ_0 (closed) and μ_1 (open). Throughout this paper the following definitions are used: μ_0, level of pipette current when the channel is closed; μ_1, level of pipette current when the channel is open; $m = (\mu_0 + \mu_1)/2$, mean value between the levels; $p = (\mu_1 - \mu_0)/2$, half-jump magnitude.

Hinkley detector

The application of the Hinkley detector to patch-clamp data is explained in detail in a previous article (Schultze and Draber, 1993). Briefly, the Hinkley detector builds a cumulative sum $g(t)$ from the measured time series $z(t) - m$:

$$g(t) = g(t - T_s) + (z(t) - m) \cdot T_s \qquad (6)$$

with the sampling period T_s. This test value $g(t)$ is not allowed to obtain negative values. This is the essential nonlinearity of the algorithm. A jump (opening or closure) is detected when the test value $g(t)$ exceeds a threshold λ.

$$\lambda = t_{res} \cdot p \qquad (7)$$

The threshold λ depends on the time resolution t_{res}, which in turn has to be chosen according to the noise magnitude (see Eq. 1). For this theoretical treatment we do not explicitly include noise into the differential equations, but we assume a time resolution $t_{res} > 0$.

In this article, we use a continuous-time version of the Hinkley detector. The difference equation (Eq. 6) becomes a differential equation. When the detector is in the state of

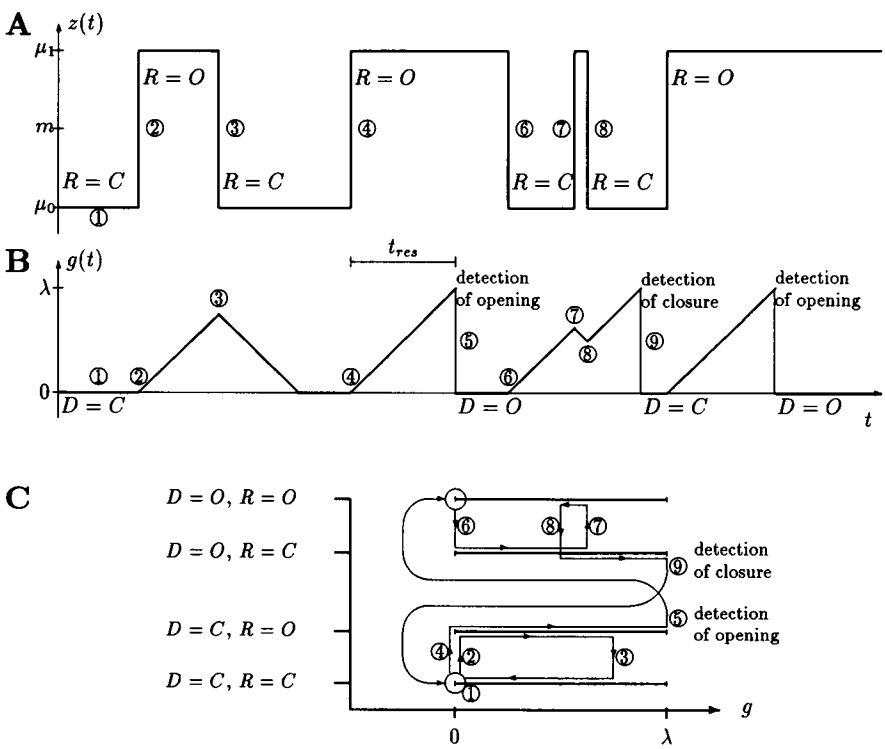

FIGURE 1 Example of the temporal behavior of the channel and the detector. Some important moments of time are marked by numbers (①, ②, etc.). (*A*) A noise-free time series $z(t)$ of pipette current jumping between closed state ($R = C$, $z(t) = \mu_0$) and open state ($R = O$, $z(t) = \mu_1$). (*B*) State of the detector characterized by the test value $g(t)$ and the detected state D (open or closed) according to the time series (*A*). (*C*) The four thick horizontal lines represent the state space for the whole system consisting of channel and detector. The horizontal dimension is the continuous state variable g. The vertical dimension stands for the four combinations of discrete states ($D = O$, $R = O$; $D = O$, $R = C$; $D = C$, $R = O$; $D = C$, $R = C$), with R being the state of the channel and D the state of the detector. The arrows and the numbers indicate the state of the system moving around in its space, according to the time series shown in *A* and *B*. On the uppermost and the lowest state line, the detector has recognized the correct state of the channel ($D = R$). Therefore, the system state moves left with constant speed $-p$ until reaching the circles $g(t) = 0$. On the two lines in the middle the detector has not yet detected the correct state of the channel and the system state moves right with constant speed p. When g finally reaches the threshold λ and a jump is detected, the detector has again recognized the state of the channel. Jumps from one line to another occur when either the channel changes its state or the detector changes its state due to jump detection.

assuming a closed channel and is therefore looking for an opening, the test value $g(t)$ of the detector behaves according to the differential equation

$$\text{Detector closed:} \quad \frac{dg(t)}{dt} = z(t) - m \tag{8}$$

as long as $g(t) \geq 0$, but $g(t)$ is not allowed to become negative. If $g(t) = 0$ and $z(t) < m$, the test value $g(t)$ stays at zero (nonlinearity). This is normally the case when the channel is closed (① in Fig. 1). When the channel opens (②), the test value starts to rise with a slope of

Detector closed, channel open:

$$\frac{dg(t)}{dt} = z(t) - m = \mu_1 - m = p \tag{9}$$

If the open event is longer than t_{res}, the test value keeps on growing until it finally reaches the threshold $\lambda = p \cdot t_{res}$, which is the criterion for jump detection. If, however, the channel closes before a jump is detected (③ in Fig. 1), the test value begins to decay with the negative slope

Detector closed, channel closed:

$$\frac{dg(t)}{dt} = z(t) - m = \mu_0 - m = -p \tag{10}$$

If the channel stays closed, the test value $g(t)$ will reach $g(t) = 0$ again. A missed event like this is displayed at the left (② and ③) of the time series in Fig. 1. The second open event (④ and ⑥) in Fig. 1 is longer than the time resolution t_{res}, the threshold λ is exceeded, and the opening is detected (⑤). From now on the detector is assuming an open channel and is searching for a closure. The test value is calculated in the same manner but with inverse signs

$$\text{Detector open:} \quad \frac{dg(t)}{dt} = m - z(t) \tag{11}$$

The next events in Fig. 1 *A* are two short closed events interrupted by an even shorter open event. The test value rises, falls, and rises again (⑥, ⑦, and ⑧ in Fig. 1 *B*). A closure is detected (⑨) although both closed events are shorter than the time resolution. This is an example of the errors arising in previous approaches from the simple assumption that a detector ignores all events shorter than t_{res}.

System state: channel and detector

The state of the whole system of channel and detector is described by the continuous test value $g(t)$ and by two discrete variables, one for the real or true state $R(t) = O$ or $R(t) = C$ of the channel and one for the state $D(t) = O$ or $D(t) = C$ of the detector. The characterization of the four combinations ($R = O, D = O$ as detected open; $R = O, D = C$ as missed open; $R = C$, $D = O$ as missed closed; and $R = C$, $D = C$ as detected closed) goes back to Blatz and Magleby (1986) and was generalized by Crouzy and Sigworth (1990). The new idea of our approach is the additional continous variable $g(t)$ for the description of the system state. In a graphical presentation (Fig. 1 *C*) the state of the whole system can be understood as a point moving in a state space which consists of four g-lines, one line for each combination of discrete states.

Probabilities in the state space

For finding the relationship $\tau_o(k_{oc}, k_{co}, t_{res})$, we chose to calculate the mean dwell time $M_o = \tau_o + t_{res}$ in the state $D = O$. This apparent mean open-time is related to the number of closures detected per time:

$$M_o = \tau_o + t_{res} = \frac{\text{time spent in } D = O}{\text{number of detected closures}} \tag{12}$$

In order to determine the number of detections we want to know the probability of the system to be in the state $(D = O, R = C, g = \lambda)$ because this is the state directly before a closure is detected.

This problem can only be solved within a more general question: What is the probability of finding the system at time t at any location R, D, g in the state space (Fig. 1 *C*)? Later on, we can remove the time dependence by focusing on stationary probability densities, and we find that it is sufficient to calculate the probabilities under the condition that the detector assumes open ($D = O$). We restrict the following considerations only to the upper two lines in Fig.1 *C* ($D = O$). Under this condition tree locations of the system state are distinguished:

1. If the channel has been open long enough, i.e., the assumption of the detector is correct, in that case the system state stays at $D = O$, $R = O$, $g = 0$. This is due to the nonlinearity of the Hinkley detector which prevents g from becoming negative. The sytem state is found at the $g = 0$-circle on the $(D = O, R = O)$-line in Fig. 1 *C* with the probability $w_{g=0}(t)$ (between ⑤ and ⑥ in Fig. 1 *C*).
2. If the channel is closed ($R = C$), i.e., the assumption $D = O$ of the detector is wrong, the system state is moving to the right on the $(D = O, R = C)$-line between $0 < g < \lambda$. $w_c(g, t)$ describes the probability density of finding the system state at time t at the location g on the $(D = O, R = C)$-line (between ⑥ and ⑦ or ⑧ and ⑨ in Fig. 1 *C*).
3. For the channel being open and $0 < g < \lambda$, the system state is moving to the left on the $(D = O, R = O)$-line. We define the probability density function $w_o(g, t)$ (between ⑦ and ⑧ in Fig. 1 *C*).

The functions w_o and w_c are probability densities and not dwell-time histograms. The sum of all probabilities for $D = O$

$$w_{g=0}(t) + \int_0^\lambda w_c(g, t)\, dg + \int_0^\lambda w_o(g, t)\, dg = w_{D=O}(t) < 1 \tag{13}$$

gives the total probability of the detector being in the open

state ($D = O$). Of course, the same argument can be applied to the other two lines ($D = C$) in Fig. 1.

Temporal evolution

The probabilities and probability densities have been introduced in order to deal with the stochastic system in a deterministic fashion. Although the system is stochastic, the temporal evolution of the probability distributions is deterministic. We are dealing with a Markov model, and the temporal evolution of the probabilities depends only on the actual probabilities. Given the probabilities and the probability densities at a moment of time t, the future development $dw_{g=0}/dt$, $\partial w_c/\partial t$, $\partial w_o/\partial t$ is determined by deterministic differential equations.

There are three fluxes that account for changes of the probability densities $w_o(g, t)$ and $w_c(g, t)$: 1) movement along the g-lines with constant speed p or $-p$; 2) openings of the channel; and 3) closures of the channel. First, we restrict our considerations to the deterministic movement of the system state on the g-lines with constant speed p (Eq. 9) or $-p$ (Eq. 10). On the $(D = 0, R = C)$-line in Fig. 1 *C*, the system state moves right with speed p. Not considering the switching of the channel, the probability density $w_c(g, t)$ moves right, too. Given a certain value $w(g_1, t_1)$ at time t_1 and location g_1, the movement of the whole density function shifts it to $g_2 = g_1 + p \cdot \Delta t$ at time $t_2 = t_1 + \Delta t$:

Without effect of gating:

$$w_c(g_2, t_2) = w_c(g_1, t_1) \tag{14}$$

$$w_c(g_1 + p\Delta t, t_1 + \Delta t) = w_c(g_1, t_1) \tag{15}$$

After some rearrangement

$$\frac{w_c(g_1 + p\Delta t, t_1 + \Delta t) - w_c(g_1 + p\Delta t, t_1)}{\Delta t} = -\frac{w_c(g_1 + p\Delta t, t_1) - w_c(g_1, t_1)}{\Delta t} \tag{16}$$

it is possible to let $\Delta t \to 0$. If the partial derivatives exist, the right moving probability density w_c is described by the following partial differential equation (PDE)

Without effect of gating:

$$\frac{\partial w_c(g_1, t_1)}{\partial t} = -p\frac{\partial w_c(g_1, t_1)}{\partial g} \tag{17}$$

There are two other effects that influence the temporal evolution $\partial w_c/\partial t$. The stochastic openings (⑦ in Fig. 1) cause a flux $-k_{co}w_c$ from w_c to w_o and decrease the probability density w_c. The closures (⑧) produce a flux $k_{oc}w_o$, which increases w_c. The final PDE for the temporal evolution of the probability density w_c therefore is

$$\frac{\partial w_c(g, t)}{\partial t} = -p\frac{\partial w_c(g, t)}{\partial g} - k_{co}w_c(g, t) + k_{oc}w_o(g, t) \tag{18}$$

The PDE for w_o is constructed similarly. The only difference is that now the state moves left with speed $-p$ instead of p:

$$\frac{\partial w_o(g, t)}{\partial t} = p\frac{\partial w_o(g, t)}{\partial g} + k_{co}w_c(g, t) - k_{oc}w_o(g, t) \tag{19}$$

Such a PDE, which describes a state of discrete and continous nature, is called the Fokker-Planck-Kolmogorov type (FitzHugh, 1983).

Further on, we need the differential equation for $dw_{g=0}/dt$. The decrease due to channel closure (⑥) is $-k_{oc}w_{g=0}$. There are two sources of increase, the flux $pw_o(0, t)$ of the distribution w_o into the point $g = 0$ (nonlinearity of the Hinkley detector) and the influx due to detection of openings (⑤).

$$\frac{dw_{g=0}(t)}{dt} = -k_{oc}w_{g=0}(t) + pw_o(0, t) + \text{influx due to detection of opening} \tag{20}$$

Finally, two continuity equations serve as boundary conditions for the PDEs: the flux $pw_c(\lambda, t)$ over the threshold λ is the efflux due to detection of closures (⑨).

$$\text{Efflux due to detection of closure} = pw_c(\lambda, t) \tag{21}$$

The channel closures from $g = 0$ (⑥) supply the flux $pw_c(0, t)$ at the left end of the $(R = C, D = O)$-line:

$$pw_c(0, t) = k_{oc}w_{g=0}(t) \tag{22}$$

Stationary solution

The stationary solution of the partial differential equations is found by replacing the temporal derivatives by zero. In the stationary case the efflux and influx due to jump detection must be equal.

$$\text{Influx due to detection of opening} = \text{efflux due to detection of closure} \tag{23}$$

The differential equations for the stationary solution $w_o(g)$, $w_c(g)$, $w_{g=0}$ are:

From Eq. 18:

$$0 = p\frac{dw_o(g)}{dg} + k_{co}w_c(g) - k_{co}w_o(g) \tag{24}$$

From Eq. 19:

$$0 = -p\frac{dw_c(g)}{dg} - k_{co}w_c(g) + k_{co}w_o(g) \tag{25}$$

From Eqs. 20, 21, 23:

$$0 = -k_{oc}w_{g=0} + pw_o(0) + pw_c(\lambda) \tag{26}$$

From Eq. 22:

$$pw_c(0) = k_{oc}w_{g=0} \tag{27}$$

For $k_{oc} \neq k_{co}$ the general solution of Eqs. 24 to 27 with the free constant a is

$$w_c(g) = \frac{a}{k_{co} - k_{oc}}\left[k_{co}\exp\left(\frac{\lambda - g}{p}(k_{co} - k_{oc})\right) - k_{oc}\right] \quad (28)$$

$$w_o(g) = \frac{a}{k_{co} - k_{oc}}\left[k_{co}\exp\left(\frac{\lambda - g}{p}(k_{co} - k_{oc})\right) - k_{co}\right] \quad (29)$$

$$w_{g=0} = \frac{a}{k_{co} - k_{oc}} \cdot \frac{p}{k_{oc}}\left[k_{co}\exp\left(\frac{\lambda}{p}(k_{co} - k_{oc})\right) - k_{oc}\right] \quad (30)$$

In contrast to Eq. 13 we normalize $w_{D=O} = 1$ because the following calculations for τ_o make use of conditional probabilities, conditioned on $D = O$. Normalization to

$$\int_0^\lambda w_c(g)\,dg + \int_0^\lambda w_o(g)\,dg + w_{g=o} = 1 \quad (31)$$

fixes a to

$$a = \frac{k_{co} - k_{oc}}{p}\left[-\frac{2k_{co}}{k_{co} - k_{oc}}(1 - \exp(t_{res}(k_{co} - k_{oc}))) - t_{res}k_{oc} - t_{res}k_{co} + \frac{k_{co}}{k_{oc}}\exp(t_{res}(k_{co} - k_{oc})) - 1\right]^{-1} \quad (32)$$

where λ is already replaced by $p \cdot t_{res}$ (Eq. 7).

Mean dwell time in $D = O$

Since the probabilities are already conditioned on $D = O$ (Eq. 31), we can now calculate the apparent mean dwell time $M_o = \tau_o + t_{res}$ (Eq. 12) in the open state as the inverse of the efflux $w_c(\lambda) \cdot p = a \cdot p$ due to jump detection from $D = O$ to $D = C$:

$$\tau_o + t_{res} = \frac{1}{w_c(\lambda) \cdot p} = \frac{1}{a \cdot p} = \frac{1}{k_{co} - k_{oc}} \cdot \left[-\frac{2k_{co}}{k_{co} - k_{oc}}(1 - \exp(t_{res}(k_{co} - k_{oc}))) - t_{res}k_{oc} - t_{res}k_{co} + \frac{k_{co}}{k_{oc}}\exp(t_{res}(k_{co} - k_{oc})) - 1\right] \quad (33)$$

Time constant of the exponential fit

Thus, the final solution for the time constant $\tau_o(k_{oc}, k_{co}, t_{res})$ in the open-time histogram is

$$\tau_o = \frac{1}{k_{co} - k_{oc}}\left[-\frac{2k_{co}}{k_{co} - k_{oc}}(1 - \exp(t_{res}(k_{co} - k_{oc}))) - t_{res}k_{oc} - t_{res}k_{co} + \frac{k_{co}}{k_{oc}}\exp(t_{res}(k_{co} - k_{oc})) - 1\right] - t_{res} \quad (34)$$

In order to find the solution for $k_{oc} = k_{co}$ we expand the exponential function into a Taylor series in $\Delta k = k_{co} - k_{oc}$ and let $\Delta k \to 0$. The result is

$$\tau_o = k \cdot t_{res}^2 + 1/k + t_{res} \quad (35)$$

Fig. 2 *A* shows our new theoretical result (Eqs. 34 and 35) as contour plot (lines of constant τ_o). Fig. 2 *B* gives the results of the old theory (Eq. 4) for comparison. Significant differences between Fig. 2, *A* and *B*, are found if both rate constants k_{oc} and k_{co} are fast, i.e. > 0.5 t_{res}^{-1}.

Before we proceed with the comparison between the old and the new theory, we analyze simulated signals in order to have a reference for the true dependence of τ_o on k_{oc}, k_{co}, and t_{res} under normal experimental conditions.

SIMULATION

The simulation is done in discrete time. In order to avoid errors caused by discreteness, the sampling period T_{sim} has to be chosen short enough with respect to the life times of the states of the model and with respect to the time constant of the antialiasing filter, as discussed below.

The model (Eq. 5) is transformed to discrete time by multiplying the rate constants with T_{sim}, which results in transition probabilities.

$$O \underset{T_{sim}k_{co}}{\overset{T_{sim}k_{oc}}{\rightleftharpoons}} C \quad (36)$$

The simulation of this discrete Markov model is performed step by step. At every sampling step the transition probabilities $T_{sim}k_{ij}$ from the actual state i to the other states $j \neq i$ and the probability $1 - \sum_j T_{sim}k_{ij}$ to stay in state i are considered. An identically distributed random number between 0 and 1 then determines if a transition to one of the states j is performed or if the simulated channel stays in state i. It is important to choose T_{sim} so short that the probability of leaving the actual state is always very small (<0.1 as a rule of thumb). In the simulations presented in this article, the fastest rate constant is 30.000 s^{-1} and T_{sim} = 1 μs. The probability 1 $\mu s \cdot 30.000\ s^{-1} = 0.03$ is small enough. The Monte Carlo simulation of the Markov model results in an undisturbed discrete time series of current through the channel. The single-channel current for state O has been chosen

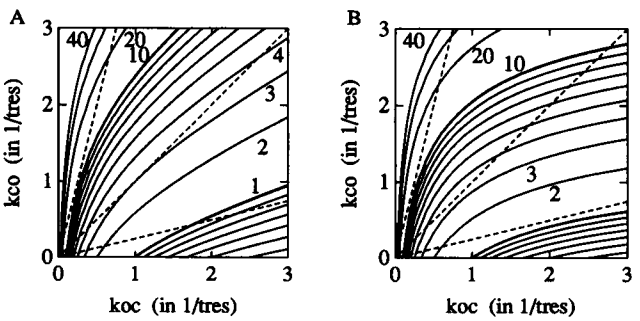

FIGURE 2 Lines of constant τ_o = 0.4, 0.5, ···, 0.9, 1, 2, 3, ···, 9, 10, 20, 30, 40 in the k_{oc}, k_{co}-plane according to (*A*) the new (Eqs. 34 and 35) and (*B*) the old (Eq. 4) theory. The dashed lines show the three cross-sections, which are examined in greater detail in Fig. 3.

to be $\mu_1 - \mu_0 = 2 \cdot p = 2.8$ pA. The time series are 20 s long, i.e., 20,000,000 simulation steps.

The typical colored noise of a patch-clamp setup is added. Its power spectrum is flat below 1 kHz and rises proportional to the frequency above 1 kHz (Colquhoun and Sigworth, 1983; Schultze and Draber, 1993). The noise amplitude after filtering and sampling is given below. Now the simulation of the unfiltered pipette current is complete. The following steps simulate the electronic processing of the measured data until they are recorded in the computer. For the low-pass filter for antialiasing we use an eighth-order Bessel filter with a cutoff frequency (-3dB) of $f_{3dB} = 25$ kHz. The discrete version is obtained by the invariant impulse-response method (Antoniou, 1979). With $f_{sim} = 1/T_{sim} = 1$ MHz $= 40 \cdot f_{3dB}$ for the simulations in this paper the errors of discretization are negligible. Generally, the simulation frequency $f_{sim} = 1/T_{sim}$ should be at least 10 times faster than the cutoff frequency f_{3dB}.

The next step of the data processing is the sampling with 100 kHz according to our laboratory setup (Schultze and Draber, 1993; Draber et al., 1993). Now the simulation of the "experimentally recorded" data is complete. The record contains 2,000,000 sampled values, the standard deviation of noise is $\sigma = 1.51$ pA, giving a signal/noise ratio SNR = 1.85. The subsequent construction of dwell-time histograms is identical to the procedure applied to real data. According to Eq. 1 the time resolution t_{res} is set to $t_{res} = 32/\text{SNR}^2 = 32/(1.85)^2 \approx 10$, sampling steps, $= 100$ μs.

For the purpose of this article we did the analysis with the three different kinds of detectors: Hinkley detector (first-order), higher order Hinkley detector, and Bessel filter with half-amplitude threshold analysis. The cutoff frequency of this Bessel filter is set to $f_{3dB} = 0.18/t_{res} = 1.8$ kHz, so that all three detectors have the same time resolution $t_{res} = 100$ μs. This "detection Bessel filter" increases the SNR to 18.9 before threshold detection. The three types of detectors and the settings of t_{res} and f_{3dB} are described in detail by Schultze and Draber (1993).

COMPARISON

In this section we compare the old Eq. 4 and the new Eq. 34 with the results from simulation and subsequent detection. We have selected three k_{oc}/k_{co} ratios (*dashed lines* in Fig. 2) for the presentation of the results: $k_{oc}/k_{co} = 4, 1, 0.25$.

Fig. 3 *A* shows the results for the fitted time constant τ_o of open events if $k_{oc}/k_{co} = 4$. Open events are then 4 times shorter than closed events; therefore, predominantly open events are missed. This has great consequences on τ_c, but not on τ_o. The time constant τ_o in Fig. 3 *A*, fitted to the open-time histogram, is less affected by missed events, because missed closed events are rare. To illustrate these arguments, we give the dotted line in Fig. 3 which stands for the inverse $1/k_{oc}$, the situation without having any missed events. The distance between the dotted line and the results (□, ○, and △) from simulation and detection is the effect of missed events. The results from the three different types of detectors, Hinkley (□), higher order Hinkley (○), and Bessel (△), are nearly identical. In the range $k_{oc} < t_{res}^{-1}$ the differences between the old theory (*dashed line*), the new theory (*solid line*), and the numerical results (□, ○, and △) are negligible. For faster

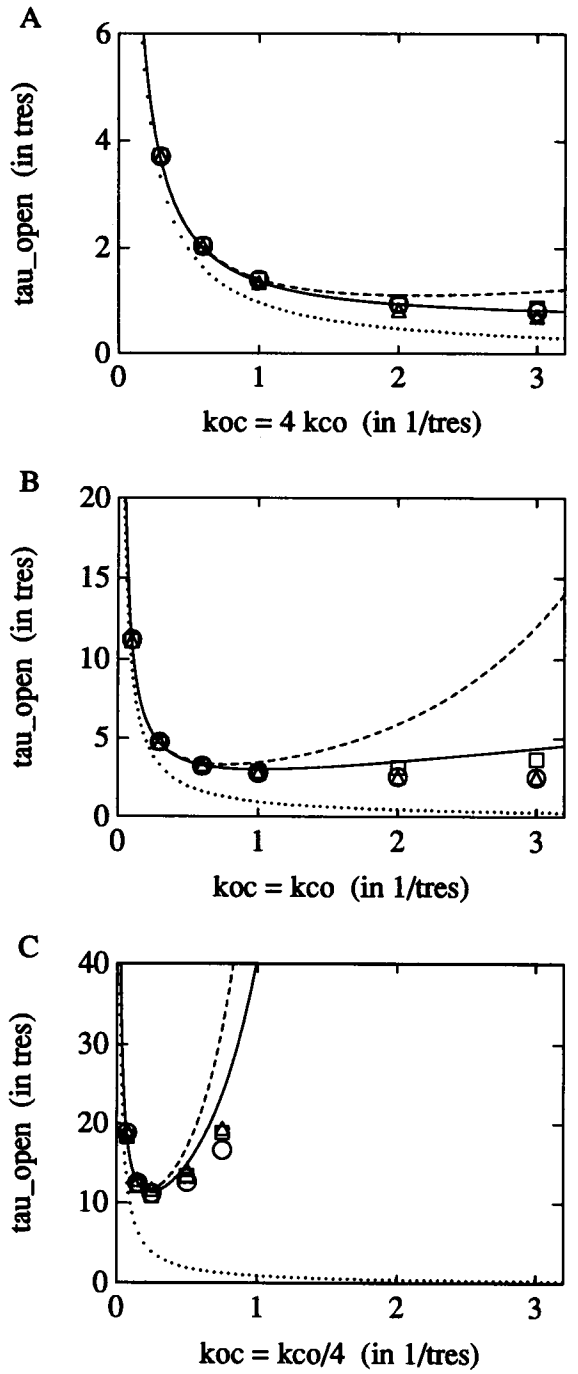

FIGURE 3 Comparison of τ_o given by the new theory (*solid line*, Eqs. 34 and 35), the old theory (*dashed line*, Eq. 4), and the $1/k_{oc}$ relationship (*dotted line*) with those obtained from the simulated time series by fitting the open-time histograms. The simulated time series were analyzed with three different detectors: Hinkley detector (□), higher order Hinkley detector (○), and Bessel filter (△). Since the time series were 2,000,000 samples long, the accuracy of the fitted time constants was very high. Repeated simulation and detection confirmed the results with less than 1% error. (*A*) $k_{oc} = 4 \cdot k_{co}$; (*B*) $k_{oc} = k_{co}$; (*C*) $k_{oc} = k_{co}/4$.

gating $k_{oc} > t_{res}^{-1}$, however, the old theory (*dashed line*) predicts a stronger effect than actually caused by missed events. The new theory (*solid line*) is still in very good accordance with the results from all three detectors.

Fig. 3 *B* compares the theoretical and numerical results for the symmetrical case $k_{oc} = k_{co}$. Closed events are now missed as often as open events. The effect of missed events, the deviations of the numerical results (□, ○, and △) from the *dotted line*, are greater than in Fig. 3 *A*. Also the differences between the detection algorithms are more obvious. When gating is very fast ($k_{oc} = k_{co} \geq 2t_{res}^{-1}$), the first-order Hinkley detector (□) gives a longer time constant τ_o than the eighth-order Hinkley detector (○) and the eighth-order Bessel filter (△). The better agreement between the new theoretical curve (*solid line*, Eq. 35) and the simulated experimental results from the Hinkley detector is no surprise since the derivation of the new theory is based on the first-order Hinkley detector. Nevertheless, the differences between the new theory (*solid line*) and the true results (□, ○, and △) are small and become obvious at very fast gating only. The old theory (*dashed line*, Eq. 4) shows serious deviations already at $k_{oc} = k_{co} = t_{res}^{-1}$. Note that both theoretical curves go through minima, which play an important role for the question of invertibility, discussed below. In both cases the deviations between theory and simulation appear on the right-hand side of the respective minimum.

In Fig. 3 *C* the effect of missed events is very strong. The situation $k_{oc} = 0.25\ k_{co}$ is complementary to Fig. 3 *A*. Now the open events are rarely missed and thus τ_o is predominantly affected by the missed closed events. All theoretical and simulated results show a minimum near $0.25\ t_{res}^{-1}$. At greater k_{oc} the apparent lifetime in the open state steeply increases because of more and more missed closed events. Interestingly, in Fig. 3 *C* the Bessel filter (△) produces more missed events than the other detectors which is in contrast to the results of Fig. 3 *B*. This is plausible because in the symmetrical case the mean of the Bessel-filtered current signal is exactly the half-amplitude threshold; therefore, the threshold is often crossed due to a short event which makes the Bessel filter also very sensitive to disturbances. In Fig. 3 *C*, however, the mean value is close to the open level, and short events are not detected so easily.

In all three cases that are shown in Fig. 3, the new theory (Eqs. 34 and 35) is in much better agreement with the experimental results from the simulations. Especially in Fig. 3 *B* with equally short open and closed events the new equation gives much a better prediction of the simulated experimental results.

DISCUSSION

Modeling a detector

The crucial point in the derivation of a formula for missed-events correction is to find an adequate model for the detector. To say that all events shorter than t_{res} are not detected is a very simple model. It leads to relatively simple analytic equations (see Eq. 4), but it is only adequate if the probability of two or more subsequent short events is negligible.

In this paper we present a more complex model for the detector. The continuous-time first-order Hinkley detector offers the possibility of modeling the "memory" of a detector, represented here by the test variable g. This feature allows the introduction of the effect of multiple short events. Thus, the dominant error of the simple model is removed. The introduction of a memory is the important new feature. Obviously, the special type of the memory is of less importance. This explains that Eq. 34 also holds for other detectors, as shown in Fig. 3.

What is neglected?

It has to be admitted, however, that there are still four minor sources of difference between the model of the detector used in the theory and a real detector used for the analysis of real or simulated patch-clamp data.

1. One normally uses a higher order detector, either the Bessel filter combined with half-amplitude threshold analysis or the higher order Hinkley detector (Schultze and Draber, 1993). Using the common eighth-order versions of these algorithms for a theoretical treatment leads to an eight-dimensional state-space instead of the one-dimensional one in Fig. 1 *C*. The partial differential equations would become much more complicated and are no longer expected to be solved analytically. Fig. 3, however, shows that the higher order Hinkley detector and the Bessel filter give results very similar to the Hinkley detector. The new Eq. 34 also fits the higher order results satisfactorily.

2. The detectors are discrete-time versions because they have to be applied to sampled data. Any formula taking into account the discrete nature of the signals will have the drawback that the sampling frequency will enter the equation as an additional parameter. Such an algorithm could not simply replace the old Eq. 4.

3. The noise is expected to have an influence on the results. White noise could be introduced into Eqs. 18 to 22 by additional terms of second-order derivatives. The introduction of the typically colored noise spectrum would, however, lead to a higher dimension of the state space. We have compared results from simulations with noise and without noise at the same t_{res} setting and found that the differences are small compared to the errors mentioned before. This is due to the noise-dependent choice of t_{res}. The noise is already indirectly taken into account via t_{res}. The new method remains valid at any amplitude of noise provided t_{res} is chosen long enough according to Eq. 1.

4. The Hinkley detector and the higher order Hinkley detector estimate the jump moment to be the last moment before jump detection with $g = 0$. The estimated jump lies before its detection. Our theoretical derivation deals directly with the moments of jump detection instead. The behavior of the detector is modeled correctly, but the estimated event lengths are a little different. Simulations have shown that the effect of this difference on the time constants is small.

The list of neglected details serves to clarify our theoretical approach. Their consequences on numerical results are very small as can be seen in Fig. 3.

Invertibility

A very important issue for practical application is the question of invertibility because the time constants are known from the experiment and the rate constants have to be determined. In Fig. 3 *B* or Eq. 35 with symmetrical rate constants, the problem is reduced to one dimension. Because of the minimum at $k = 1/t_{res}$ the whole function $\tau(k, t_{res})$ is not invertible. Given a $\tau > 3t_{res}$, there are always two solutions: a slow solution on the left branch and a fast solution on the right branch. From a practical point of view, it is, however, very unlikely to expect the true solution on the fast branch. In such a situation the high frequency of gating would lead to a noisy signal fluctuating around a mean value between the true levels of the open and closed channel (Heinemann and Sigworth, 1988). Fast gating looks like a reduction of the single-channel current (Draber et al., 1991). This effect would neither allow the identification of the true open level nor, as a consequence, the construction of dwell-time histograms. In other words, the existence of a dwell-time histogram makes it highly probable that the correct solution is on the slow branch. Fig. 4 shows the regions in which the "slow solution" allows inversion, now generalized to the two-dimensional case of asymmetric rate constants. The wider range of invertibility in the k_{oc}, k_{co}-plane as well as in the τ_o, τ_c-plane makes the new theory more convenient for practical use.

Aspects of application

For the analysis of single-channel data, we recommend the following approximate analysis procedure. After the construction of dwell-time histograms, a sum of exponentials is fitted to the range above $2t_{res}$, because deviations from the exponential shape caused by dwell-time omission only affect the range between 0 and $2t_{res}$ (Blatz and Magleby, 1986). The number of required exponentials is a lower boundary for the number of open and closed states in the gating scheme. In many practical cases the following prerequisites are fulfilled. Brief events are only produced via the fastest $O - C$ gateway in the gating scheme. These two states provide the shortest time constants in the dwell-time histogram. The exchange between this flickering pair of states and the other long-living states in the scheme is slow compared to the time resolution. The probability of missing a burst, a sojourn in the flickering pair of states, is negligible, and the probability of missing a dwell-time in the other long-living states is negligible, too. If all these prerequisites are fulfilled, it is sufficient to correct the transitions between the two flickering states, as if they were a two-state model. Select the shortest open-time constant τ_o and the shortest closed-time constant τ_c and, by numerical inversion of Eq. 34, determine the rate constants k_{oc} and k_{co} between the states *O* and *C* of the flickering gateway. The remaining slow time constants can then be treated conventionally, without missed-events correction. In a previous study we used this approach to analyze the effects of cooperative mode shifting on the rate constants (Draber et al., 1993).

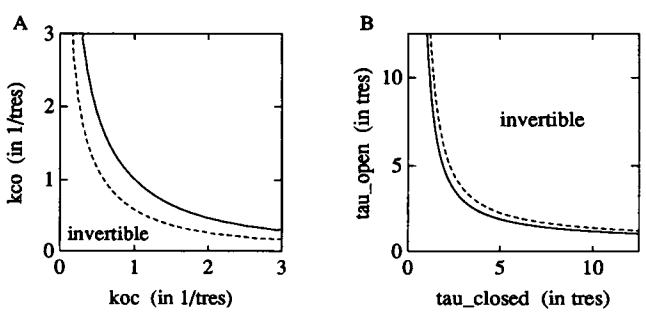

FIGURE 4 Invertibility regions of the new theory (*solid line*, Eqs. 34 and 35) and the old theory (*dashed line*, Eq. 4). (*A*) in the k_{oc}, k_{co}-plane. (*B*) in the τ_o, τ_c-plane. The new theory is invertible within a wider range.

The recommendations in this section show how to apply our new method of missed-events correction to many practical relevant cases. However, we must admit that the theory based on the fixed dead time approach is more elaborate, and solutions are available for any kind of gating model. If the model studied is very complex and the gating is not too fast (probability of two subsequent brief events less than 10%), the fixed dead time approach may be preferable for now. If, however, the gating is fast (rate constants greater than $0.5 \cdot t_{res}^{-1}$), the errors of the fixed dead time theory are no longer tolerable and our new Eq. 34 should be used.

In all cases, whatever methods have been applied, checking the result by a final simulation is useful. A single simulation takes considerably less time than fitting by repeated simulations (Magleby and Weiss, 1990). Comparing measured and simulated dwell-time histograms (Draber et al., 1993) makes sure that nothing essential has been neglected.

Future extensions of the theory

This paper gives principal analytical equations for a realistic approach to missed-events correction. To make the application to complex models with many states more straightforward, it seems to be a promising approach to study the combined Markov model (channel and detector) in the framework of the semi-Markov theory provided by Ball et al. (1993). In addition to complex gating schemes, it should be possible to account for noise (item 2 above) and for the distinction between jump detection and jump time estimation (item 4 above).

CONCLUSION

When a general equation for missed events which works independent of the type of detector and of the kind and strength of the noise is required, the new Eq. 34 for missed events is superior to the old one (Eq. 4). It is in much better

agreement with the simulated results (Fig. 3), and it has a wider range of invertibility (Fig. 4). Since the number of parameters is exactly the same we do not expect any problems when replacing the relationship between τ and k by our new one in the software for patch-clamp analysis.

We thank Prof. Dr. U.-P. Hansen, Dipl.-Phys. Christian Ruge, and Mr. Thilo Rießner for helpful discussions.

REFERENCES

Antoniou, A. 1979. Digital Filters: Analysis and Design. McGraw-Hill, New York. 129–130, 168–171.

Ball, F. G., G. F. Yeo, R. K. Milne, R. O. Edeson, B. W. Madsen, and M. S. P. Sansom. 1993. Single ion channel models incorporating aggregation and time interval omission. *Biophys. J.* 64:357–374.

Basseville, M., and A. Benveniste, editors. 1986. Detection of Abrupt Changes in Signals and Dynamical Systems. Springer-Verlag, Berlin.

Blatz, A. L., and K. L. Magleby. 1986. Correcting single channel data for missed events. *Biophys. J.* 49:967–980.

Colquhoun, D., and A. G. Hawkes. 1982. On the stochastic properties of bursts of single ion channel openings and of clusters of bursts. *Philos. Trans. R. Soc. Lond. B Biol. Sci.* 300:1–59.

Colquhoun, D., and F. J. Sigworth. 1983. Fitting and statistical analysis of single channel records. *In* Single-Channel Recording. B. Sakmann and E. Neher, editors. Plenum Press, New York. 191–263.

Crouzy, S. C., and F. J. Sigworth. 1990. Yet another approach to the dwell-time omission problem of single-channel analysis. *Biophys. J.* 58: 731–743.

Draber, S., R. Schultze, and U.-P. Hansen. 1991. Patch-clamp studies on the anomalous mole fraction effect of the K^+-channel in cytoplasmic droplets of *Nitella:* an attempt to distinguish between a multi-ion single-file pore and an enzyme kinetic model with lazy state. *J. Membr. Biol.* 123: 183–190.

Draber, S., R. Schultze, and U.-P. Hansen. 1993. Cooperative behavior of K^+ channels in the tonoplast of *Chara corallina. Biophys. J.* 65: 1553–1559.

FitzHugh, R. 1983. Statistical properties of the asymmetric random telegraph signal with application to single-channel analysis. *Math. Biosci.* 64:75–89.

Hamill, O. P., A. Marty, E. Neher, B. Sakmann, and F. J. Sigworth. 1981. Improved patch-clamp techniques for high-resolution current recording from cells and cell-free membrane patches. *Pflügers Arch. Eur. J. Physiol.* 391:85–100.

Hawkes, A. G., A. Jalali, and D. Colquhoun. 1990. The distribution of the apparent open times and shut times in a single channel record when brief events cannot be detected. *Philos. Trans. R. Soc. Lond. A Math. Phys. Sci.* 332:511–538.

Heinemann, S. H., and F. J. Sigworth. 1988. Open channel noise. IV. Estimation of rapid kinetics of formamide block in gramicidin A channels. *Biophys. J.* 54:757–764.

Hinkley, D. V. 1971. Inference about the change-point from cumulative-sum-tests. *Biometrika.* 57:1–17.

Jalali, A., and A. G. Hawkes. 1992. The distribution of the apparent occupancy times in a two-state Markov process in which brief events cannot be detected. *Adv. Appl. Probab.* 24:288–301.

Kienker, P. 1989. Equivalence of aggregated Markov models of ion-channel gating. *Proc. R. Soc. Lond. B Biol. Sci.* 236:269–309.

Klieber, H.-G., and D. Gradmann. 1993. Enzyme kinetics of the prime K^+ channel in the tonoplast of *Chara*: Selectivity and inhibition. *J. Membr. Biol.* 132:253–265.

Liebovitch, L. S. 1993. Interpretation of protein structure and dynamics from the statistics of the open and closed times measured in a single ion-channel protein. *J. Stat. Phys.* 70:329–337.

Magleby, A. L., and D. S. Weiss. 1990. Estimating kinetic parameters for single channels with simulation. A general method that resolves the missed event problem and accounts for noise. *Biophys. J.* 58:1411–1426.

Milne, R. K., G. F. Yeo, B. W. Madsen, and R. O. Edeson. 1989. Estimation of single channel kinetic parameters from data subject to limited time resolution. *Biophys. J.* 55:673–676.

Page, E. S. 1955. A test for a change in parameter occurring at an unknown point. *Biometrika.* 42:523–527.

Rickard, J. T. 1977. The zero-crossing interval statistics of the smoothed random telegraph signal. *Info. Sci.* 13:253–268.

Roux, B., and R. Sauvé. 1985. A general solution to the time interval omission problem applied to single channel analysis. *Biophys. J.* 48:149–158.

Sakmann, B., and E. Neher, editors. 1983. Single-Channel Recording. Plenum Press, New York.

Schultze, R., and S. Draber. 1993. A nonlinear filter algorithm for the detection of jumps in patch-clamp data. *J. Membr. Biol.* 132:41–52.

Yellen, G. 1984. Ionic permeation and blockade in Ca^{2+}-activated K^+ channels of bovine chromaffin cells. *J. Gen. Physiol.* 84:157–186.

Yeo, G. F., R. K. Milne, R. O. Edeson, B. W. Madsen. 1988. Statistical interference from single channel records: two-state Markov model with limited time resolution. *Proc. R. Soc. Lond. B Biol. Sci.* 235:63–94.